In: Exploratory Analysis and Data Modeling in Functional Neuroimaging, edited by F. Sommer and A. Wichert, MIT Press, Cambridge, MA, 195-207 (2002)

Having your voxels and timing them too?

Scott Makeig, 1, 2

Tzyy-Ping Jung, 2

Terrence J. Sejnowski, 1,2,3

1. Computational Neurobiology Laboratory, The Salk Institute for Biological Studies, La Jolla CA 92037
2. Institute for Neural Computation, University of California San Diego, La Jolla CA 92093
3. Howard Hughes Medical Institute

The two major noninvasive functional human brain imaging modalities developed during the last part of the twentieth century, high-density scalp EEG (electroencephalogram) and fMRI (functional magnetic resonance imaging), appear from a logical viewpoint to be largely complementary. BOLD (blood oxygen level difference) signals can have a spatial resolution of less than 1 cm^3, meaning time series of blood oxygenation level differences can be recorded from many more than 10,000 spatially and structurally identifiable brain regions (voxels). However, changes in blood oxygenation are inherently slow, much slower than the firing of individual neurons (circa 1 ms) or the frequencies at which neural networks tend to synchronize (1-200 Hz or more). EEG signals, on the other hand, can be recorded at sampling rates of a kHz or more per channel, and can thus easily and accurately record cortical potentials throughout their frequency range, if they reflect a sufficient amount or density of synchronous activity within cortex that the summed local fields reach the scalp without canceling one another. It therefore seems easy to argue, as many researchers have, that by concurrently recording EEG and fMRI BOLD signals, researchers could acquire functional brain activity data with both high spatial and high temporal resolution.

Certainly there are formidable technical problems that researchers wishing to make such concurrent recordings must overcome. Any ferromagnetic metal inside the scanner can be dangerous for the subject, and will certainly cause unacceptable loss in the BOLD image. Then too, even very small movements of the electrodes or cables in a very strong magnetic field must induce artifactual currents. The RF pulses used in fMRI scanning are another serious challenge; their sharp gradients can induce volts of current in EEG leads that usual analog EEG high pass filters will

convert into 'railed' amplifier signals. The slightest movement of the subject's scalp, including the pulse of blood through it, will move the electrodes sufficiently to produce large ballistocardiogram signals that may obscure the underlying brain activity. Finally -- or not finally, as the list of potential recording problems is long -- the sharp loud noise produced by the gradient pulses several times a second may generate large auditory evoked responses or induce more general perturbations of the field dynamics in the brain of the subject.

However, even after having dealt with or overcome all these and related problems, it is important to reconsider whether promoting EEG and BOLD signals as "complementary" in space and time is not too glib a concept. EEG is, first and foremost, an index of local cortical synchrony. EEG signals, certainly, reflect synchronous dendritic and possibly glial activity within domains of cortical tissue (neuropile) much much larger than a single neuron, most probably within hypercolumn-scale or larger domains. Perhaps 'neuropile synchrony' is a better term, if one gives room for active contributions of inhibitory neural networks (with their electrotonic as well as synaptic couplings) and for active contributions of non-neural glial networks. Blood oxygenation, on the other hand, is considered to index the brain response to local metabolic need in the neuropile, mediated and controlled by mechanisms whose details are not yet understood.

Since EEG and BOLD signals reflect different phenomena -- spatial synchronization and total metabolic consumption, respectively -- EEG and BOLD signals, even from the same patch of cortex, may be as unrelated to each other as are phase and amplitude in Fourier spectra of random signals. *That is, there is no a priori reason to assume they have any correlation at all*! Before assuming a direct relationship between EEG and BOLD signals, we must answer the following question: *Do synchronized neuronal excitatory and inhibitory processes demand more oxygen than the same processes in a desynchronized state?* The largest normal EEG rhythms, after all, occur in deepest sleep stages, when overall brain metabolic demands (and most BOLD signals) are somewhat lower than during waking. Lack of a firm answer to this question should give us pause, and leads inevitably to the conclusion that making *a priori* assumptions about the interrelationship of EEG and BOLD signals is foolish in advance either of direct experimental evidence (from adequate concurrent EEG / fMRI studies) and/or more detailed understanding of their biophysics.

Even less well founded, in our view, are assumptions espoused by many researchers that BOLD signal increases following sensory stimuli are highly likely to indicate the brain areas responsible for generating small features (e.g., peaks) of averaged event-related potentials (ERPs) evoked by the same stimuli. We believe the very nature of the ERP may be different from that assumed by most researchers. The usual conception is the idea that sensory-evoked ERPs sum

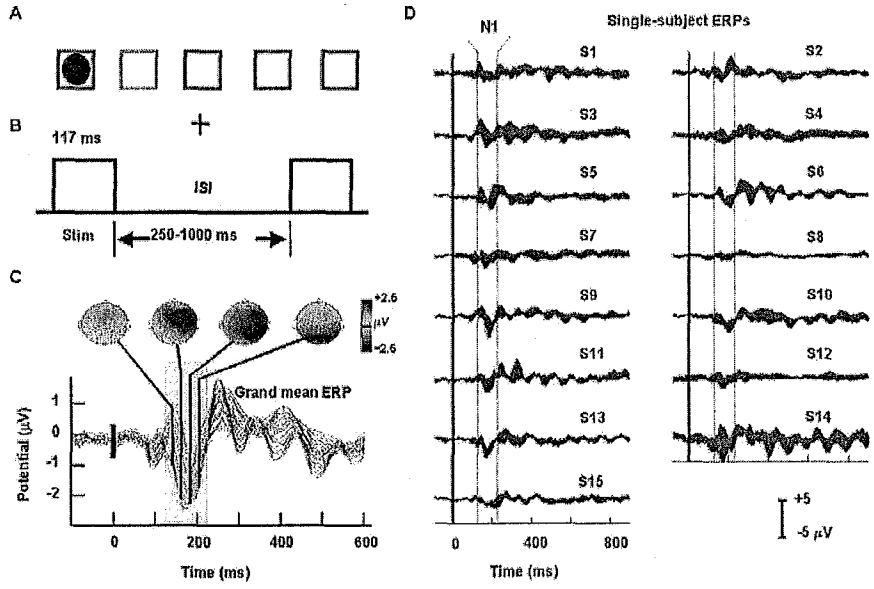

Fig. 1. Visual Nontarget Stimulus-Evoked ERPs. (A) Screen display for the spatial selective attention experiment. Five 1.6 cm^2 square outlines indicating possible stimulus locations were permanently displayed 0.8 cm above a central fixation cross. In each 76-s block of trials, one outline was colored green, indicating the target location for that block of trials. Target location was evenly distributed over the five stimulus locations across 30 trial blocks per subject. **(B)** Stimulus timing. Stimuli were briefly flashed white circular discs each presented for 117 ms in a randomly selected stimulus location following a randomly selected inter-stimulus interval of 250 to 1000 ms. Subjects were asked to press a right thumb button press as quickly as possible each time a (target) stimulus appeared in the target location (green box), and to ignore (nontarget) stimuli presented in the other four boxes. **(C)** Averaged responses from 15 subjects (S1-S15). EEG data were collected from 29 scalp plus two periocular sites, referred to the right mastoid at a rate of 256 Hz/channel with an analogue band pass of 0.01 to 100 Hz. Scalp impedances were kept below 5 kΩ. After rejecting epochs containing out-of-bounds values, data were low pass filtered below 40 Hz to suppress line noise. Averaged responses to nontarget stimuli presented to the left of fixation (mean trials per subject, 922). Grand mean of 15 single-subject ERPs time locked to the brief appearance of the disk in a non-attended box to the left of subject fixation. The light blue area marks the defined N1 response interval (50 ms before and after the RMS N1 peak). The four interpolated scalp maps show the shifting scalp distribution of the averaged response during the N1 interval. Following the N1 feature, circa 10-Hz rhythmic activity appears in the evoked response. Fig. 2B shows that this 'alpha ringing' does not arise from an increase in 10-Hz energy in the EEG. **(D)** Envelopes of the 15 single-subject ERPs. The solid blue response envelopes enclose the individual response traces for all 29 scalp channels. Vertical dashed lines mark the grand mean N1 interval.

monodirectional potentials accompanying and indexing phasic stimulus-induced increases in neural firing rates observed in some neurons within limited, cytoanatomically-defined sensory cortical processing areas. In general, however, positive and negative peaks in averaged ERP waveforms may not index changes in total EEG energy time locked to stimulus onset, such as can be measured in the time/frequency domain by the ERSP (event-related spectral perturbation) method (Makeig, 1993). Instead, most features of averaged ERPs may be produced by event-related perturbations in the phase statistics of ongoing EEG activity (Makeig et al., 2002).

Many event-related increases in EEG spectral amplitudes, on the other hand, (as seen in ERSP plots) are *not* correlated with the reliable appearance of positive or negative potential peaks in the raw EEG time series. Such a correlation may occur only when the increases in EEG energy take the form of bursts that are reliably (1) time locked (e.g., peaking at the same latency, relative to event onset, across trials) and (2) phase locked (e.g., exhibiting the same phase at the same latency.

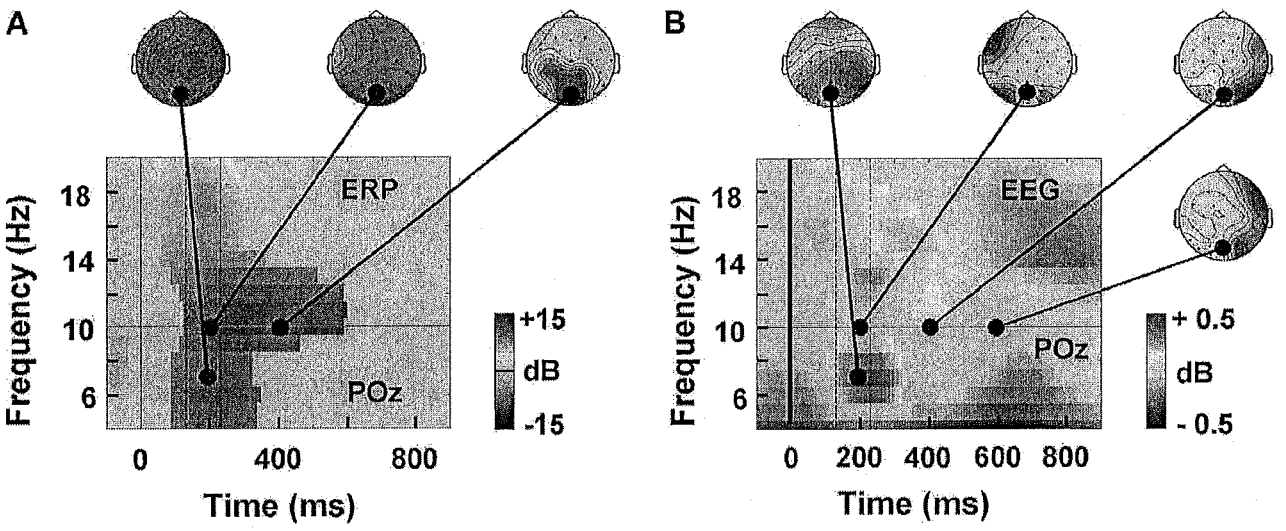

Fig. 2. Differences between Event-related Power Spectral Changes in the ERP and EEG.. (A) Event-related spectral perturbation (ERSP) plot showing mean post-stimulus increases in spectral power of the single-subject ERPs, averaged across 15 subjects. Shaded areas in the time/frequency plane that show significant ($p < .02$) post-stimulus increases or decreases (see color scale) in log spectral power in the averaged ERP waveform at a central parietal electrode site (POz) relative to mean power in the averaged 1-s pre-stimulus ERP. Topographic scalp maps show topography of the post-stimulus power increases in the ERP across all 29 scalp channels at three indicated points in the time/frequency plane. (B) Event-related spectral perturbations (ERSPs) for the unaveraged EEG at central posterior site POz following left visual field nontarget stimulus presentations. Mean of similar time/frequency transforms 15 subjects. Log spectral power at each time and frequency was normalized by subtracting mean log power in the 1-s pre-stimulus baseline. Features near (7 Hz, 200 ms) and (16 Hz, 350 ms) reflect small power increases. Vertical dotted lines, the N1 interval; horizontal line, 10 Hz. Cartoon heads, scalp topographies of differences in spectral amplitude, relative to baseline, at the indicated time-frequency points.

and central burst frequency) to the experimental events of interest. For example, following onset of briefly flashed, left-hemifield non-target squares (cueing no subject response) in a special selective attention experiment we observed a small (0.5 dB) event-related increase in EEG power near 7 Hz (Fig. 2B), whereas the ERP waveforms showed a much larger (15-dB) post-stimulus increase in spectral power which was prolonged near 10 Hz (Fig. 2A). Furthermore, the scalp topographies over which the two increases occurred were dissimilar.

Even increases in EEG spectral amplitudes (irregardless of phase) cannot be assumed to correlate with BOLD signal increases. This is clearly shown by two recent preliminary reports of negative and positive correlations, respectively between BOLD signals and EEG amplitudes in the alpha and gamma bands, respectively (Goldman et al., 2001; Logothetis et al., 2001).

EEG signals are produced by spatial synchronization of electrochemical activity in cortex; ERPs by synchronization of EEG signals time locked to the occurrence of some class of experimental events. Recently, we have shown that the electroencephalographic (EEG) response to a small visual stimulus presented in an unattended location in a selective spatial attention task (Fig. 1) is better modeled by stimulus-induced phase realignment of EEG activity within domains of strong cortical synchrony that appear to generate most of the ongoing EEG (Makeig et al., 2002) (Fig. 2). These EEG domains need not be located within single functionally-defined cortical processing areas. Some evidence suggests they may extend across boundaries between such areas (Rogeul-Buser et al., 1997). If visual ERPs are produced by stimulus-induced phase resetting of multiple ongoing EEG processes rather than by consistent evoked positive or negative potentials generated in restricted cortical areas, as strongly supported by our results and other reports as early as Sayers et al. (1974), it appears naïve to assume that generators of single ERP peaks should be co-located with areas of significant event-related BOLD signal change. BOLD signal changes should reflect changes in the level of neural or neuroglial activity in local cortical domains whose size is determined by the voxel size of the measurement (convolved with hemodynamic control patterns). Even if some ERP peak were generated predominantly in a single compact cortical area, it is premature to assume that a relatively slow BOLD signal increase should be triggered by a brief period of net positive or negative far-field potential, as this might well reflect a transient increase in synchronization of synaptic activity rather than an increase in its metabolic activity level.

If the time courses of averaged ERPs do not accurately reflect event-related dynamic patterns in the unaveraged EEG signals, which may in turn differ in complex ways from trial to trial, then combining averaged BOLD and EEG/ERP data collected in separate sessions is an idea built on shaky ground indeed. Here we report results of a single-subject, single-channel pilot study to test the feasibility of recording and analysis of concurrent EEG and BOLD data. Preliminary results from this study were reported earlier (Jung et al., 1999).

Methods. EEG epochs time locked to presentation of an RF pulse during an oddball/rare-target "P300" experiment at the vertex to a flashed target shape (in the fovea), from a pilot experiment conducted . The data (232 trials) were collected during continuous, concurrent EPI scanning using a

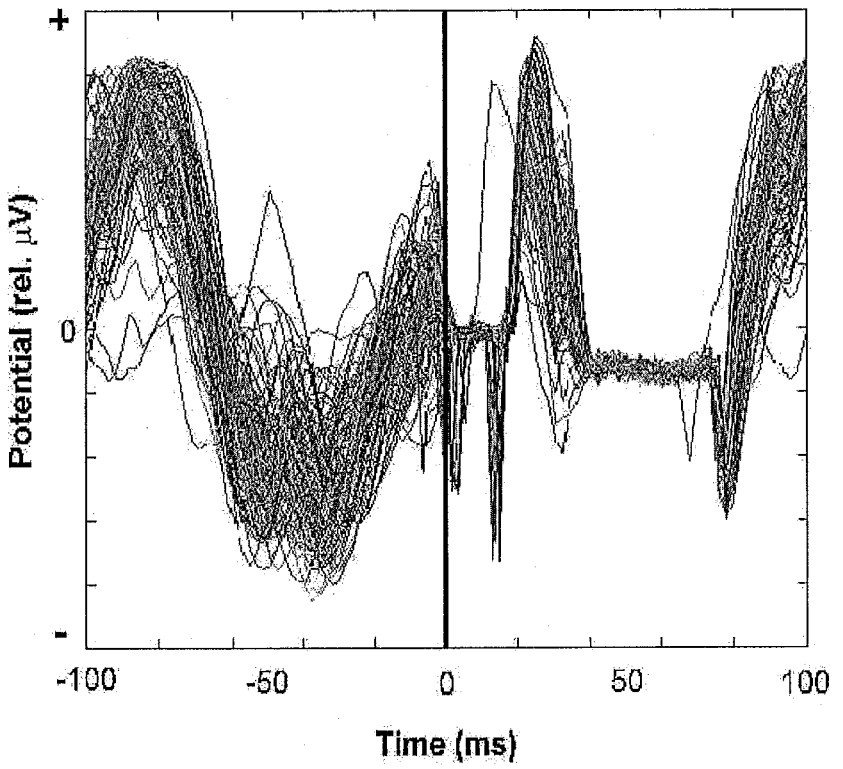

Fig. 3. Scan-related EEG artifact. One hundred consecutive EEG epochs time locked to the onset (at time 0) of RF pulses during fMRI scanning. The ~80 msec timeout period is followed/preceded by a stereotyped noise waveform.to which is added EEG variability occurring during the ~120 msec non-blanking periods. Removing the mean pulse-locked artifact from each pulse epoch allows reconstructing the variable EEG and ERP activity in single trials (see Figs. 2-3). Y-axis scaling is proportional to μV.

Siemens 1.5-T scanner at a rate of 5 slices per second in a blocked paradigm consisting of three 4-minute bouts each consisting of 40-s task blocks consisting of presentations of standard circles (75%) and target squares (25%)) alternating with 40-s control blocks during which the nontarget stimuli only were presented and the subject was instructed only to continue to fixate a dot at screen center while ignoring the flashed stimuli. Stimulus SOAs ranged between 435 and 1116 ms. During task blocks the adult volunteer subject was asked to attend to differences between the visual stimuli and to push a handheld button as soon as possible after presentation of a target (square) stimulus. The subject wore earplugs to minimize sound from the scanner during scanning pulses. Behavioral responses to targets were collected via a non-metallic thumb button held in the subject's right hand. EEG was recorded from a tin electrode placed over the right central scalp and referenced to another placed over the right mastoid. The electrodes were attached to the amplifier by carbon wire (Electrocap, Inc.). The recording used an analog pass band of 0.1-30 Hz and a sampling rate of 500 Hz. The amplifier (SA Instrumentation, Inc.) was especially constructed to operate on batteries placed before and after an optical bridge, and to 'time out' during a pulse produced by the Siemens scanner from a few ms before to approximately 16 ms after the production of each RF scanning pulse. During these brief time-out periods, capacitors held the EEG signal level nearly constant to minimize switching artifacts.

EEG Artifact Removal. First, the mean noise waveform time locked to the RF pulse was removed from the data. The relative consistency of this noise is indicated by Fig. 3, which shows EEG epochs time-aligned to 100 consecutive RF pulses using a relative microvolt scale. Unfortunately, for this pilot experiment microvolt calibrations were not available. Time 0 marks the onset of the RF pulse. The figure shows the time-out period (with 2 sharp but relatively small remaining spike artifacts), and a larger 10-Hz artifact time locked to pulse presentation. The precise origin of the 10-Hz wave is unknown -- two obvious candidates are ringing at the frequency of the scanning pulse (near 1500 Hz) aliased down to near 10 Hz by the 500-Hz EEG sampling-rate, and/or possibly, entrainment of subject alpha/mu activity by the pulse (and accompanying loud noise burst) sequence. The mean artifact was then subtracted from the EEG data surrounding each RF pulse. (Pulse onsets were recorded on a separate recording channel). Next, EEG epochs surrounded the 226 target stimulus presentations were extracted from the cleaned data and imaged using the ERP-image plotting technique (Jung et al., 1999; Makeig et al., 1999). Finally, we performed ERSP and

phase resetting analysis on the cleaned data. The figures were created using an ICA/EEG toolbox for MATLAB (The Mathworks, Inc.) available for download on the Web (sccn.ucsd.edu/eeglab/)

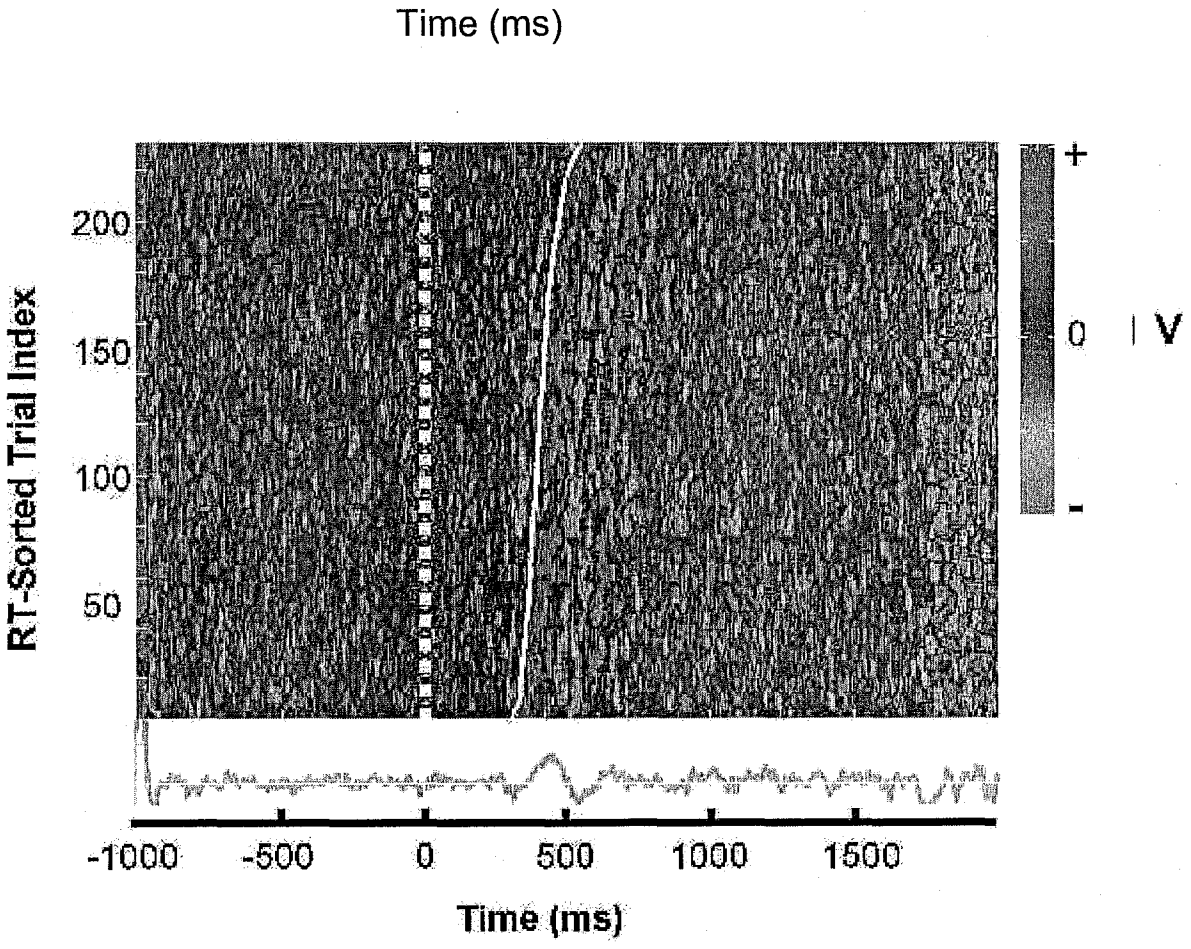

Fig. 4. Target stimulus-aligned ERP-image plot. This plot shows the 226 single trials after removing the mean pulse-locked artifacts from each trial. The dotted white line shows the stimulus onset time. The curved solid white line shows subject response time (RT) after sorting trials by RT. Both the data and the RT curve are smoothed with a 20-trial moving average. The averaged target-locked response is shown below the image of the single-trial data.

Results. Single-trial results are summarized in Fig. 4 using the 'ERP-image' plotting format (Jung et al., 1999; Makeig et al., 1999). The striate pattern visible in the pre-stimulus EEG data (and throughout) reflects the remaining pulse-locked artifact. However, as the delivery of stimuli was not time locked to the production of scanning pulses, the ERP-image format clearly reveals event-related potential activity in single trials (horizontal image lines) which here are sorted in ascending

order of response latency (indicated by the sloping white line). The cleaned data clear show the presence of a complex pattern of evoked response activity time-locked to the button press. The trace below the ERP-image shows the average ERP of the cleaned trials.

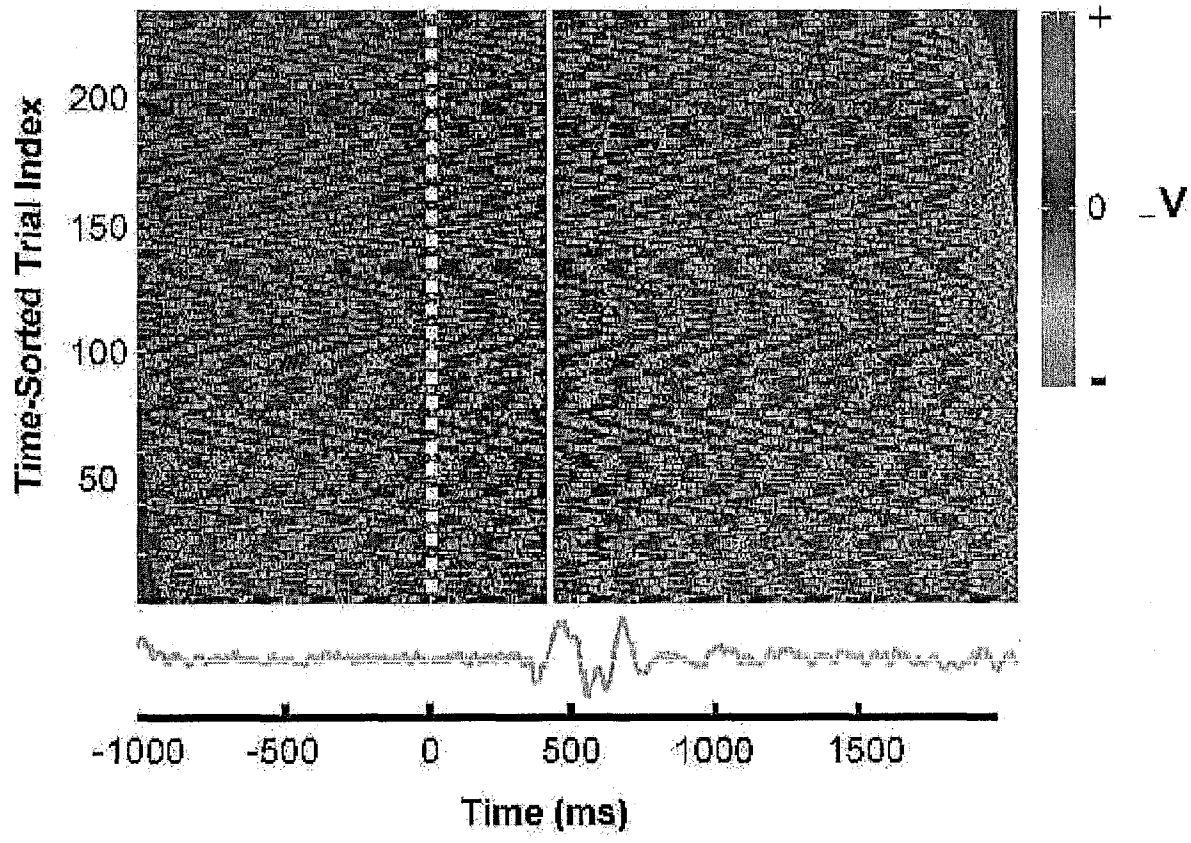

Fig. 5. Response-aligned ERP-image plot. This plot shows the 226 single trials after removing the RF-pulse artifacts from each trial. The trials are aligned to median subject reaction time (403 ms, solid white line). The dotted white line shows the median stimulus onset time. The mean RT-aligned response is shown below the single-trial image. Notice the additional small peak (after 500 ms) in the response-locked average response (lower trace); this feature does not appear in the stimulus-locked average (Fig. 4 lower trace).

As Fig. 4 clearly shows, the averaged ERP is smeared because of the relatively broad range of response times in different trials. The lower trace of Fig. 5 shows the response-locked ERP for the same trials. Note the ~10-Hz activity in the ~100 ms following the response (solid white line). This may represent the phase resetting of mu activity, as suggested by other results obtained out of the scanner. The two larger peaks of the averaged evoked response are separated by approximately 200 ms, suggesting a circa 5-Hz character.

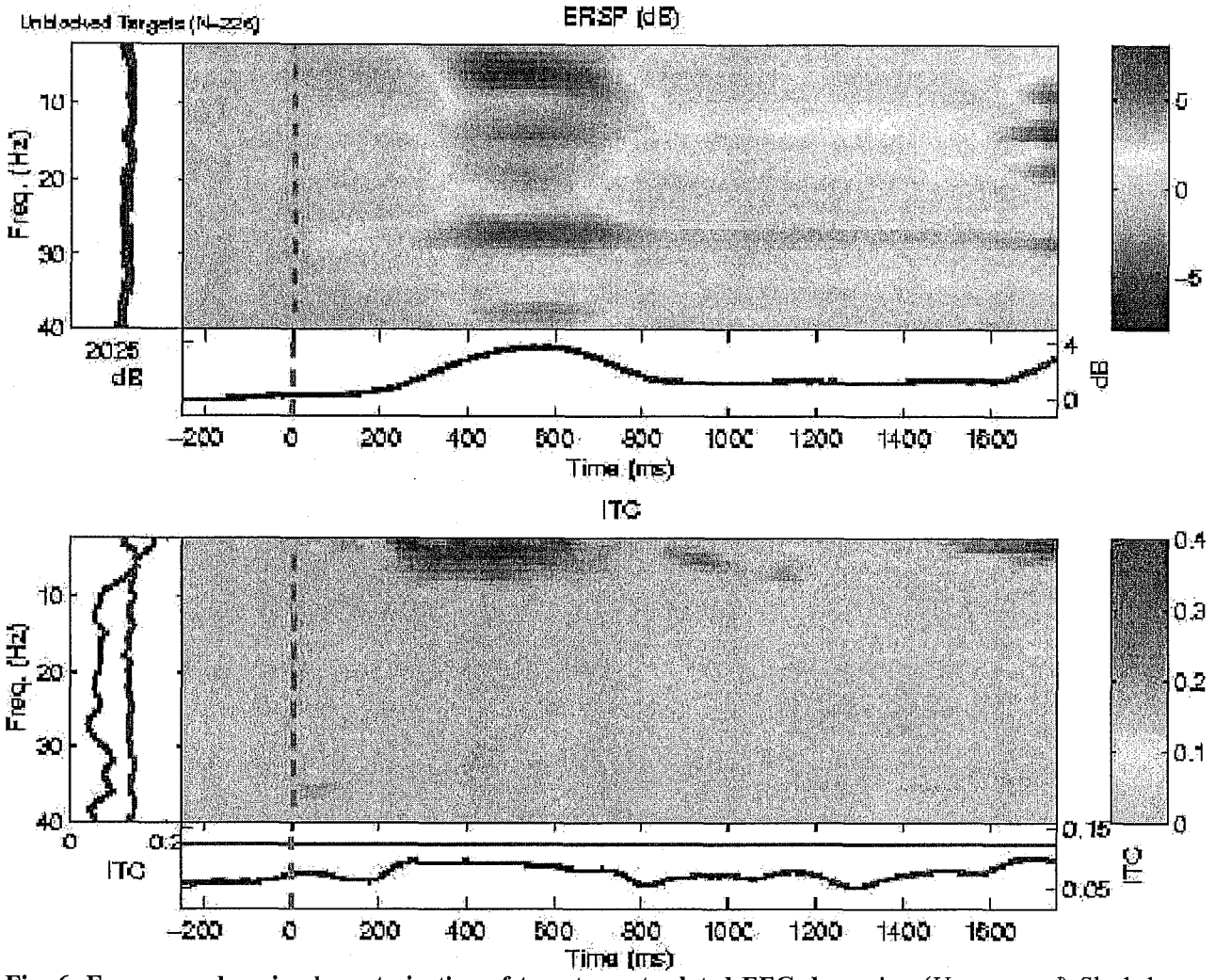

Fig. 6. Frequency domain characterization of target event-related EEG dynamics. (*Upper panel*) Shaded areas show significant transient event-related power increases in the EEG spectrum (the event-related spectral perturbation, ERSP) during the 232 target response epochs time locked to stimulus onset. In addition to the circa 4-8 Hz theta band power increase during the period of the late evoked response (400-700 ms), there are increases near 12, 19 and 38 Hz, plus a lengthy post-stimulus increase in power near 28 Hz. (Increases after 1500 ms are probably edge artifacts). (*Lower panel*) Significant changes in inter-trial coherence (ITC) measuring changes in consistency of EEG phase-locking of the EEG at each frequency to stimulus onsets. None are evident save for the ERP-related circa 4-5 Hz peak. Thus, the 28-Hz augmentation in the upper panel represents an event-related amplitude modulation of 28-Hz activity without phase resetting.

Fig. 6 presents time/frequency analysis of the same target epochs. The top panel shows the ERSP, which includes a strong (6-dB) mean increase in theta band power (near 5 Hz) in single trials during the evoked response. This theta power increase does not in itself produce the 5-Hz ERP features. Instead, as shown in the lower panel, the phase of theta bursts following the motor response is not random. This switch from a pre-stimulus random to a post-stimulus non-random phase distribution across trials, termed 'phase resetting,' is indexed by the significant (r=0.4) inter-

trial coherence in the theta band. More exactly, the term should be 'partial phase resetting,' since the resetting is incomplete ($1 >> r >> 0$).

The top panel also shows that the increase in EEG following the subject response is not confined to one frequency band. Instead, a similar though smaller phasic power increase is seen near 14 Hz, 18 Hz, and 38 Hz. Near 38 Hz, the augmentation begins just after stimulus onset and continues throughout the epoch, again peaking after the button press. The augmentations at these higher frequencies are not accompanied by phase resetting, since phase following the stimulus is random (ITC not significantly different from 0). However, Fig. 6 measures ITC relative to stimulus onset. Fig. 5 suggests significant phase resetting occurs time locked to the motor response in at least two bands (near 5 and 10 Hz). The occurrence of partial phase resetting in the theta band time locked to both the stimulus and the motor response is quite possible. Further research would be required to determine if this occurred in different trial subsets or only as a consequence of the response time distribution being concentrated in less than a 200 ms window representing one 5-Hz cycle (see Fig. 5). We are examining the relation of phase resetting to perceptual awareness and behavior in more extensive EEG-only data sets.

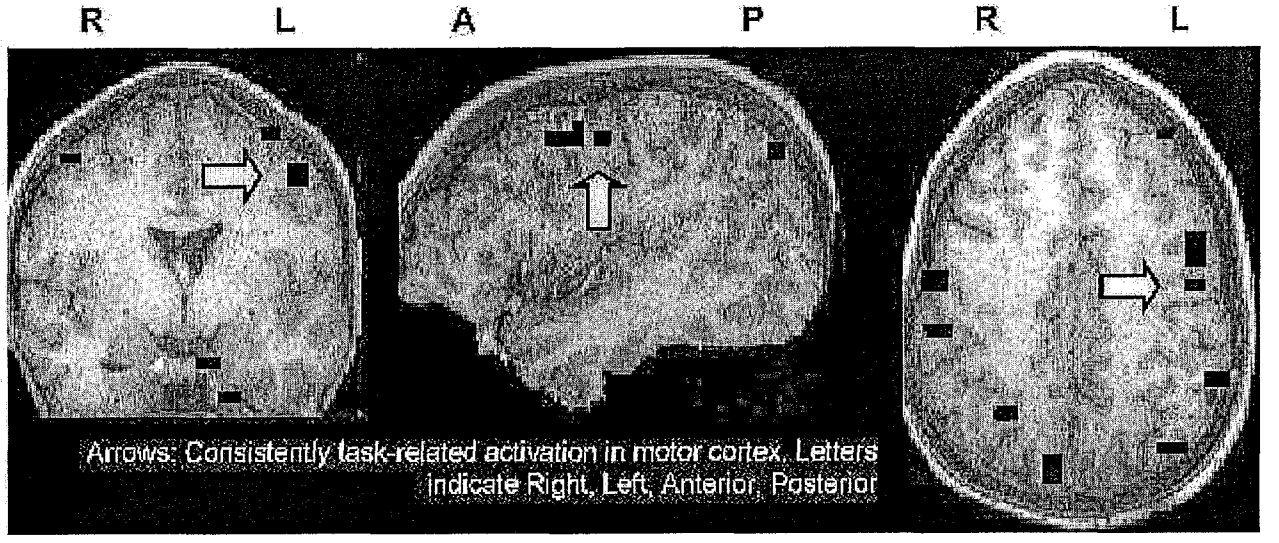

Figure 7. Voxels whose BOLD signals are positively correlated (r>0.3) with the task block design. BOLD data recorded during concurrent EEG acquisition on a Siemens 1.5-T scanner shows BOLD activation in left motor cortex during a visual detection task requiring right thumb button presses.

BOLD Signal Analysis. Straightforward correlation analysis was performed on the BOLD data by correlating its time course at each brain voxel with a task design reference function obtained by convolving the alternating block design time course with a model hemodynamic response function. Results, shown in Fig. 7, included expected activations in left motor cortex at or near the expected location hand motor area. Artifacts from the electrodes were confined primarily to supra-brain areas. Further analysis of this pilot experiment data was not attempted. Currently, we are

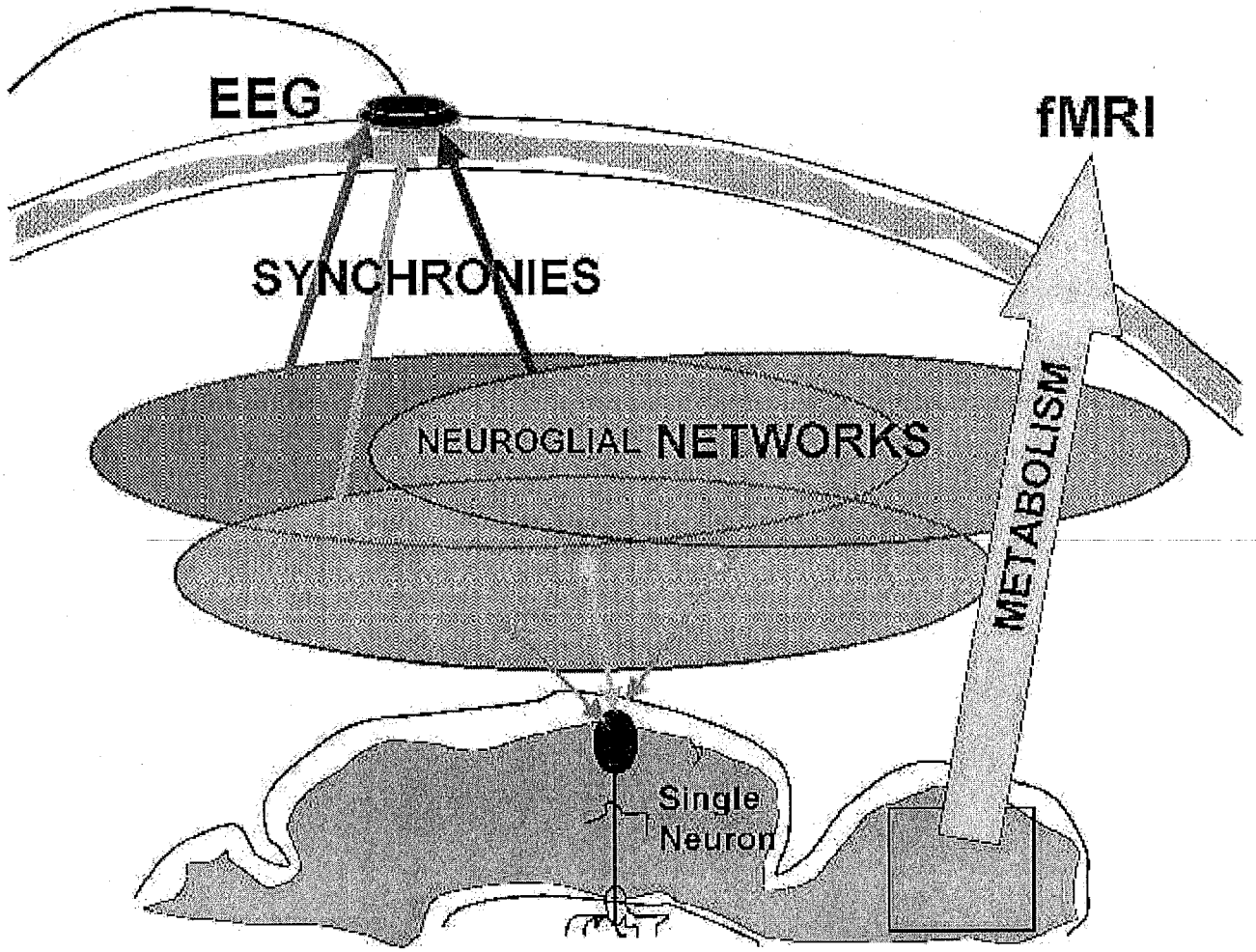

Figure 8. EEG and fMRI BOLD data measure different aspects of cortical activity. Whereas the BOLD signal is thought to measure the brain hemodynamic response to local metabolic need, the scalp EEG sums volume-conducted potentials generated in cortical domains/networks (of unknown size, shape and density) across which extracellular potential varies with sufficient synchronicity. Synchronous activity, as reflected in far-field potentials, can also modulate firing of individual neurons. Changes in the degree of synchronization of activity in a cortical area may not mirror changes in total metabolic consumption; thus changes in EEG power need not be correlated with BOLD signal changes.

performing experiments using a continuous performance task and 72 similar scalp electrodes, with an intention to compare the spatially independent components of the BOLD signals (McKeown et

al., 1998) with the dynamics of temporally independent components of the concurrently recorded EEG (Makeig et al., 1996).

Discussion

EEG signals recorded from the scalp arise through synchronous activity in cortical domains or networks. Cortical BOLD signals, on the other hand, are believed to index the brain response to total metabolic demand. In theory, these may be as uncoupled as phase and amplitude are in noise signals. As Fig. 8 also depicts schematically, single pyramidal cells in cortex can only fire upon receiving sufficient synchronous excitatory input. It is now becoming clear that synchronization of activity across and between cortical areas can effectively bias or modulate the firing of single neurons. Thus, information transfer in cortex is also controlled in part by the network synchronies that give rise to EEG. If changes in EEG power and in BOLD signal strength are significantly related, we suggest the nature of their links cannot be guessed in advance, may prove complex, and may eventually be understood to arise through biophysical mechanisms whose details are not yet discovered.

Clearly, the true test of these predictions will come from sufficient analysis of a wide range of recordings of concurrent EEG and BOLD signals. The pilot data we have shown here indicate that detailed analysis of the dynamics of concurrently recorded EEG and BOLD signals is feasible, even to the extent of single-trial analysis of human cognitive ERP features. However, we have argued that the most intimate relationship between BOLD and EEG signals is not likely to be between BOLD differences and sources of peaks in ERP scalp waveforms, as other have suggested, but between BOLD signals and changes in power and/or other whole-signal features of the scalp EEG. Early results in this direction are promising. Logothetis and colleagues (2001) have reported preliminary results from a relatively few cells in a small cortical area of anesthetized monkeys that indicate that neural firing rate may not be as *positive* a correlate of BOLD signals as is changes in the power of local field potentials in the gamma band (above 30 Hz). Goldman and colleagues (2001), however, have reported that BOLD signal levels within discrete cm-scale domains of posterior cortex in humans are *negatively* correlated with alpha band EEG power on the posterior scalp, while in other places (e.g., in insula, thalamus) the same correlation may be *positive*. Clearly,

we expect that concurrent EEG and fMRI studies will prove important for the development of cognitive neuroscience, and possibly for neuroscience in general.

Acknowledgments.

We acknowledge the essential contributions of Jeanne Townsend, Marissa Westerfield, Rick Buxton and Eric Wong of UCSD and of Gary Priebe of SA Instrimentation, Inc. in the collection of the data, as well as the financial support of the National Institutes of Health and The Swartz Foundation.

References

R. Goldman, J. Stern, J. Engel, M. Cohen, Tomographic mapping of alpha rhythm using simultaneous EEG/fMRI, Human Brain Mapping, Brighton, UK (2001).

T-P Jung, S. Makeig, J. Townsend, M. Westerfield, B. Hicks, E. Courchesne and T.J. Sejnowski. "Single-trial ERPs during continuous fMRI scanning." *Society for Neuroscience Abstracts*, 1999.

N. Logothetis, J. Pauls, M. Augath, T. Trinath, A. Oeltermann, *Nature* **412**, 150 (2001).

M. J. McKeown *et al.*, *Human Brain Mapping* **6**, 160-88 (1998).

S. Makeig, *Electroencephalogr Clin Neurophysiol* **86**, 283 (1993).

S. Makeig, A. J. Bell, T-P. Jung, T. J. Sejnowski, *Advances Neural Information Processing Systems* **8**, 145 (1996).

S. Makeig, M. Westerfield, T-P. Jung, J. Townsend, E. Courchesne, T. J. Sejnowski, *Science* 295:690-694 (2002).

A. Rogeul-Buser, P. Buser, *Int J Psychophysiolog* **26**, 191 (1997).

B. M. Sayers, H. A. Beagley, W. R. Henshall, *Nature* **247**, 481 (1974).